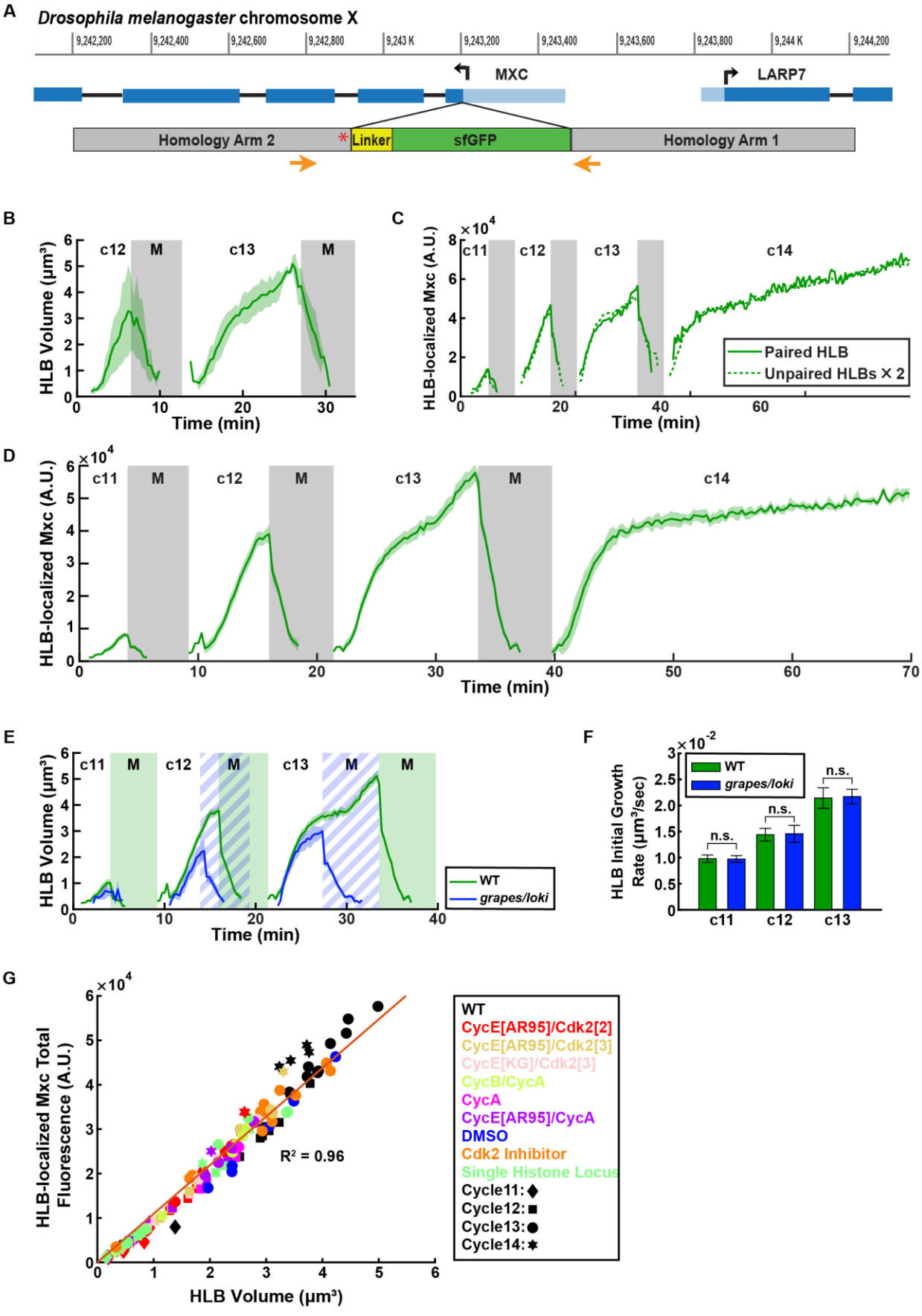
A
Drosophila melanogaster chromosome X
9,242,200
9,242,400
9,242,600
9,242,800
9,243 K
9,243,200
9,243,400
9,243,600
9,243,800
9,244 K
9,244,200
MXC
LARP7
Homology Arm 2
Linker
sfGFP
Homology Arm 1
B
HLB Volume (μm³)
c12
M
c13
M
Time (min)
C
×10⁴
HLB-localized Mxc (A.U.)
c11
c12
c13
c14
Paired HLB
Unpaired HLBs × 2
Time (min)
D
×10⁴
HLB-localized Mxc (A.U.)
c11
M
c12
M
c13
M
c14
Time (min)
E
HLB Volume (μm³)
c11
M
c12
M
c13
M
M
WT
grapes/loki
Time (min)
F
×10⁻²
HLB Initial Growth Rate (μm³/sec)
WT
grapes/loki
n.s.
n.s.
n.s.
c11
c12
c13
G
×10⁴
HLB-localized Mxc Total Fluorescence (A.U.)
R² = 0.96
HLB Volume (μm³)
WT
CycE[AR95]/Cdk2[2]
CycE[AR95]/Cdk2[3]
CycE[KG]/Cdk2[3]
CycB/CycA
CycA
CycE[AR95]/CycA
DMSO
Cdk2 Inhibitor
Single Histone Locus
Cycle11:
Cycle12:
Cycle13:
Cycle14:

Figure S1. Molecular biology and detailed analysis of HLB dynamics, Related to Figure 1
(A) Sequences encoding super folder GFP (green box) and an 18 amino acid linker (yellow box) were inserted just upstream of the *mxc* initiator methionine codon, using homology arms indicated by gray boxes. The asterisk indicates the location of the CRISPR guide RNA target site, and the orange arrows indicate primers used for PCR screening. Numbers indicate X chromosome nucleotide positions from *Drosophila melanogaster* reference genome r_6. (B) HLB size measured during cycles 12-13 for embryos with endogenously tagged GFP-Mxc. N=3 embryos. (C) Comparison between the HLB-localized Mxc total fluorescence of fused HLBs ('paired (fused) HLB') and that of two HLBs that have not fused ('unpaired HLBs multiplied by 2') for a single embryo. (D) HLB-localized Mxc total fluorescence during cycles 11-14 for WT embryos. N=10 embryos. (E) HLB size during cycles 11-13 for the *grapes/loki* (mammalian ortholog of *Chk1/Chk2*) mutants. The beginning of S phase is aligned with that of WT for comparison, as this mutant has a shorter S phase. Mitoses for the *grapes/loki* mutants are marked as striped blue area. (F) The initial growth rate of HLB for WT and *grapes/loki* mutants measured by slopes of Figure S1D. Error bars, standard deviation. n.s., not significant. (G) Correlation between HLB-localized Mxc total fluorescence (y axis) and HLB size (x axis) for various genotypes used in the study. Shaded area, SEM. n.s., not significant. A.U., arbitrary units. c, cycle. M, mitosis.

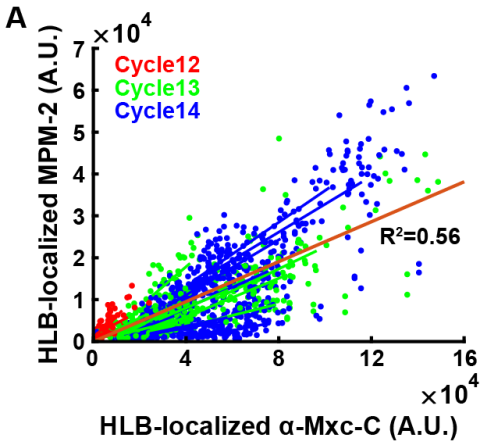

Figure S2. MPM-2 staining correlates with Mxc during S phase, Related to Figure 2
(A) Total fluorescence from the MPM-2 antibody staining and the Mxc antibody staining. Orange line is the best fit line through the origin. Each colored line is the best fit line for each embryo, in the color of its respective cycle. N=22 embryos. A.U., arbitrary units.

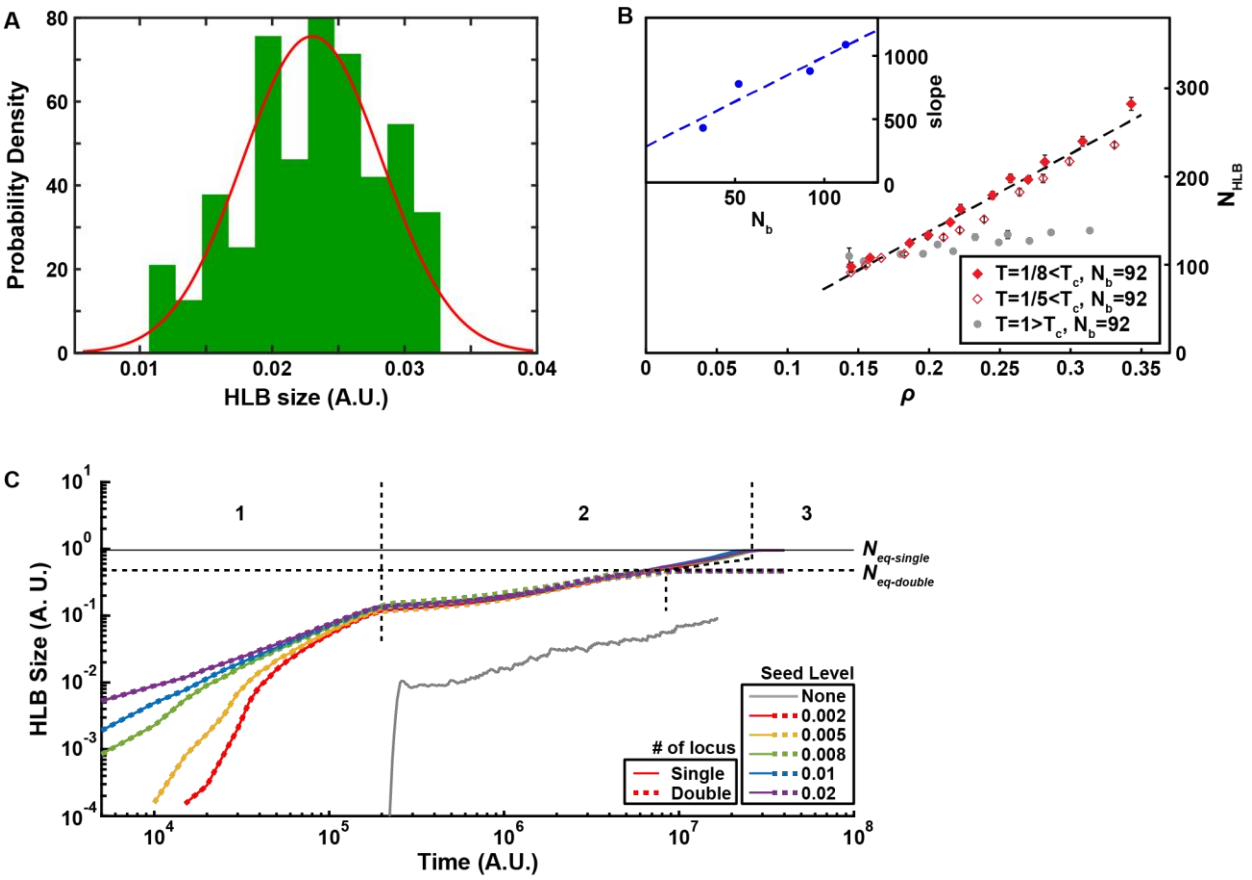

Figure S3. Additional simulation results, Related to Figure 3

(A) HLB size distribution from a simulation that includes seeding. Red line fitted Gaussian distribution. (B) Average volume of the HLB droplet, N_{HLB}, as a function of the average concentration outside the droplet ρ, after 10^5 MC steps of the model (6) on a cubic lattice of $L = 43$ sites with seeding level $N_b = 92$. Filled diamonds correspond to $T = 1/8$. Dashed lines are the linear fts of the data as $N_{HLB} = \alpha\rho+\beta$. Empty diamonds correspond to a slightly higher temperature, but still below T_c, $T = 1/5$. Gray filled circles correspond to $T = 1$, slightly above T_c. Inset: Slope α obtained from the linear fit of the main panel as a function of N_b. The main figure was $N_b = 92$, and additional points of $N_b = 32$, $N_b = 52$, and $N_b = 112$ are shown. (C) HLB growth simulation through numerical solution of Cahn-Hilliard (CH) equation in 2D lattice, with single seed locus (solid line) and double seed loci (dashed line), with different levels of seed (same as Figure 3I). $N_{eq\text{-}single}$, equilibrium size for the single seed locus simulation. $N_{eq\text{-}double}$, equilibrium size for the double seed loci simulation. A.U., arbitrary units. c, cycle. M, mitosis.

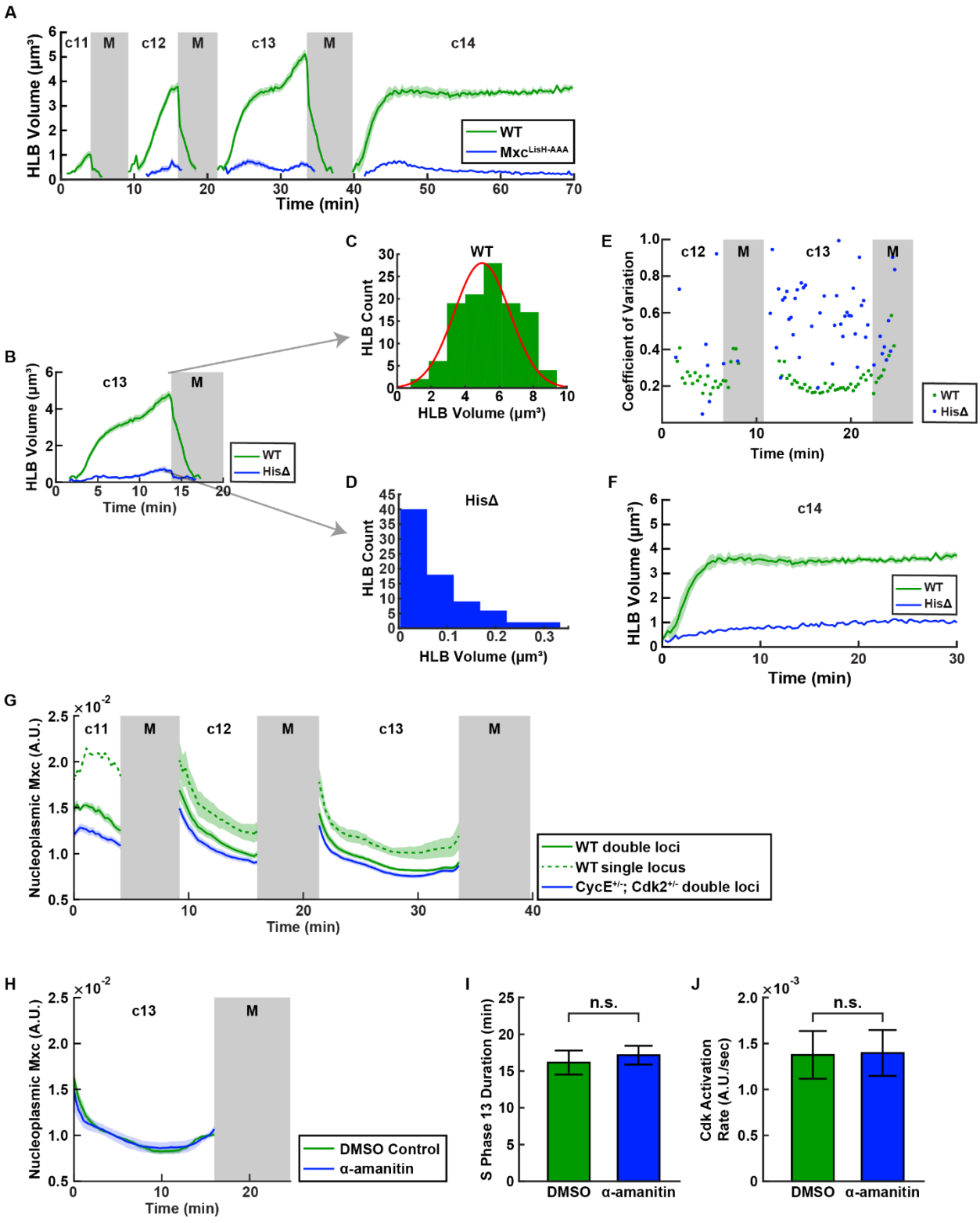

Figure S4. Additional data on Mxc$^{LisH-AAA}$ and transcriptional seeding, Related to Figure 4
(A) HLB size during cycle 11-14 for WT and *mxc$^{LisH-AAA}$* mutants. N=10 embryos (WT), 5 embryos (Mxc$^{LisH-AAA}$). (B) HLB size for WT and histone deficiency (HisΔ) embryos for cycle 13 (from Figure 4B). N=10 embryos (WT) and 12 embryos (HisΔ). Arrows indicate representative examples of

HLB size distribution for (C) WT and (D) HisΔ. (E) Comparison of HLB size coefficient of variation (CoV) for WT and HisΔ embryos. (F) HLB size for WT (N=4) and HisΔ (N=1) embryos for cycle 14. Longer S phase allows for proto-HLBs to grow to a more significant size. (G) GFP-Mxc level in the nucleoplasm over cycles 11-13 for different genotypes. N=10 (WT double loci), 9 (WT single locus), 17 embryos ($CycE^{+/-}$; $Cdk2^{+/-}$). (H) GFP-Mxc level in the nucleoplasm over cycle 13 for DMSO control (N=6) and α-amanitin injected (N=5) embryos. (I) Cycle 13 S-phase duration for DMSO control (N=6) and α-amanitin injected (N=5) embryos. (J) Cdk sensor phosphorylation level for DMSO control (N=6) and α-amanitin injected (N=5) embryos. A.U., arbitrary units. c, cycle. M, mitosis.

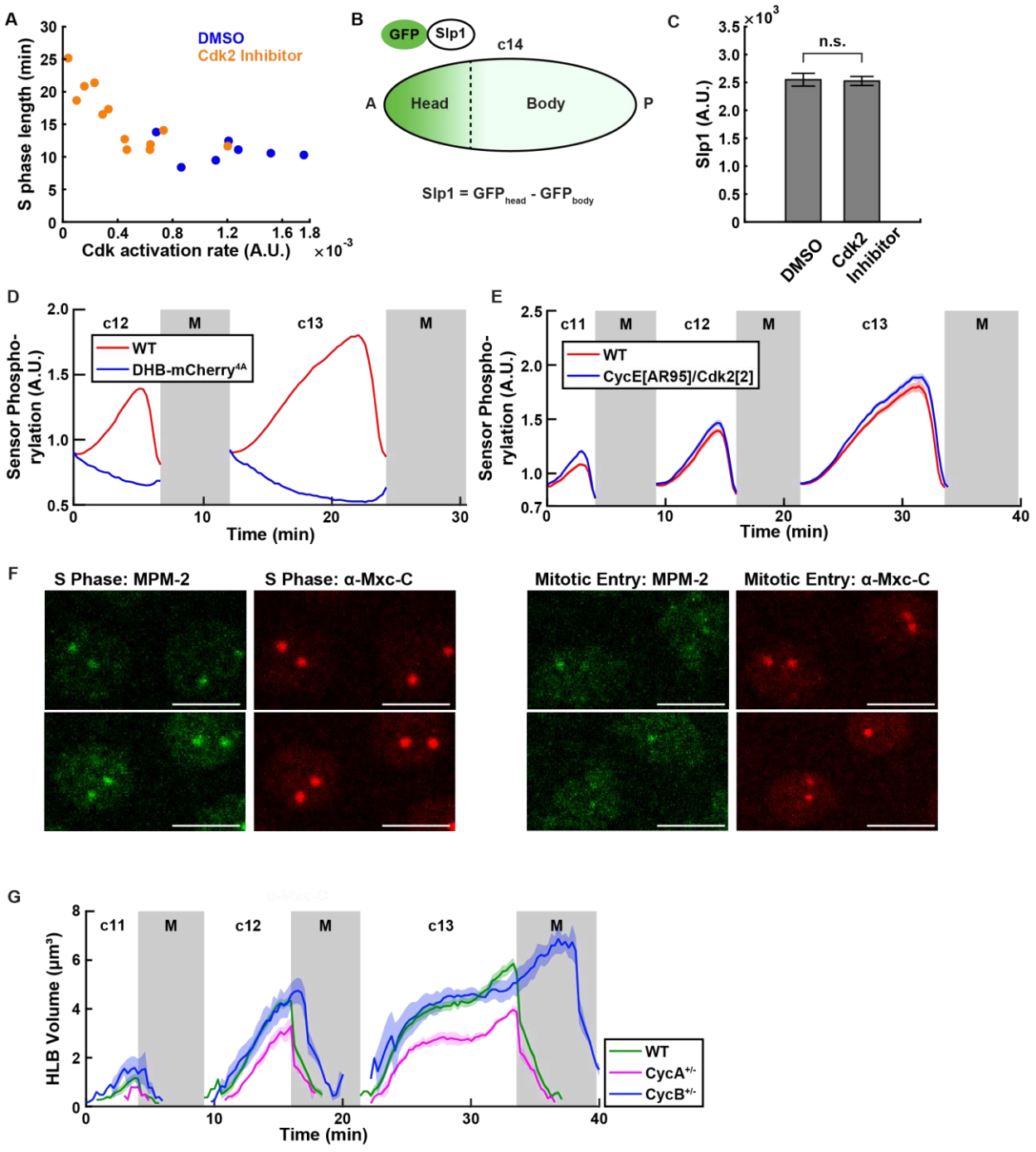

Figure S5. Regulation of S-phase Cdk phosphorylation and its effect on HLB growth, Related to Figure 5

(A) S phase length and Cdk activation readout from the Cdk sensor. (B) To investigate whether injections of SNS-032 inhibitor alter transcription by acting on Cdks other than Cdk2, we quantified the expression levels of the transcription factor sloppy paired 1 (Slp1), a zygotically expressed gene, during cycle 14. We compared the GFP-Slp1 protein for DMSO control and SNS-032-injected embryos over a period of about 4.2 minutes during cycle 14. (C) Slp1 level. Error bars, standard deviation. n.s., not significant. (D) Cdk activity measured from WT sensor (red, N=10) and the mutant sensor DHB-mCherry^{4A} (blue, N=1). (E) Cdk activity measured from the sensor

for embryos laid by WT mothers (red, N=10) and $CycE^{+/-}$; $Cdk2^{+/-}$ mothers (blue, N=17). (F) MPM-2 and an antibody against Mxc C-terminus (α-Mxc-C) staining for nuclei in S phase (left) and mitotic entry (right). The S phase staining for MPM-2 and α-Mxc-C correlate strongly (see also Figure S2 for a quantification). However, as the nuclei enter mitosis, MPM-2 foci have disappeared or have become smaller while Mxc remains inside the HLB. The decrease in MPM-2 fluorescence preceding mitosis mirrors the decrease in activity readout from the biosensor in (D), suggesting that Mxc and the DHB peptide used in the biosensor are phosphorylated/dephosphorylated with similar dynamics during the cell cycle. Scale bars, 5μm. (G) HLB size for embryos laid by WT (green, N=10), $CycA^{+/-}$ (magenta, N=3), and $CycB^{+/-}$ (blue, N=3) mothers. For comparison, the beginning of S phase for $CycB^{+/-}$ embryos was aligned with other genotypes even if they had a longer S phase. c, cycle. M, mitosis. A.U., arbitrary units.

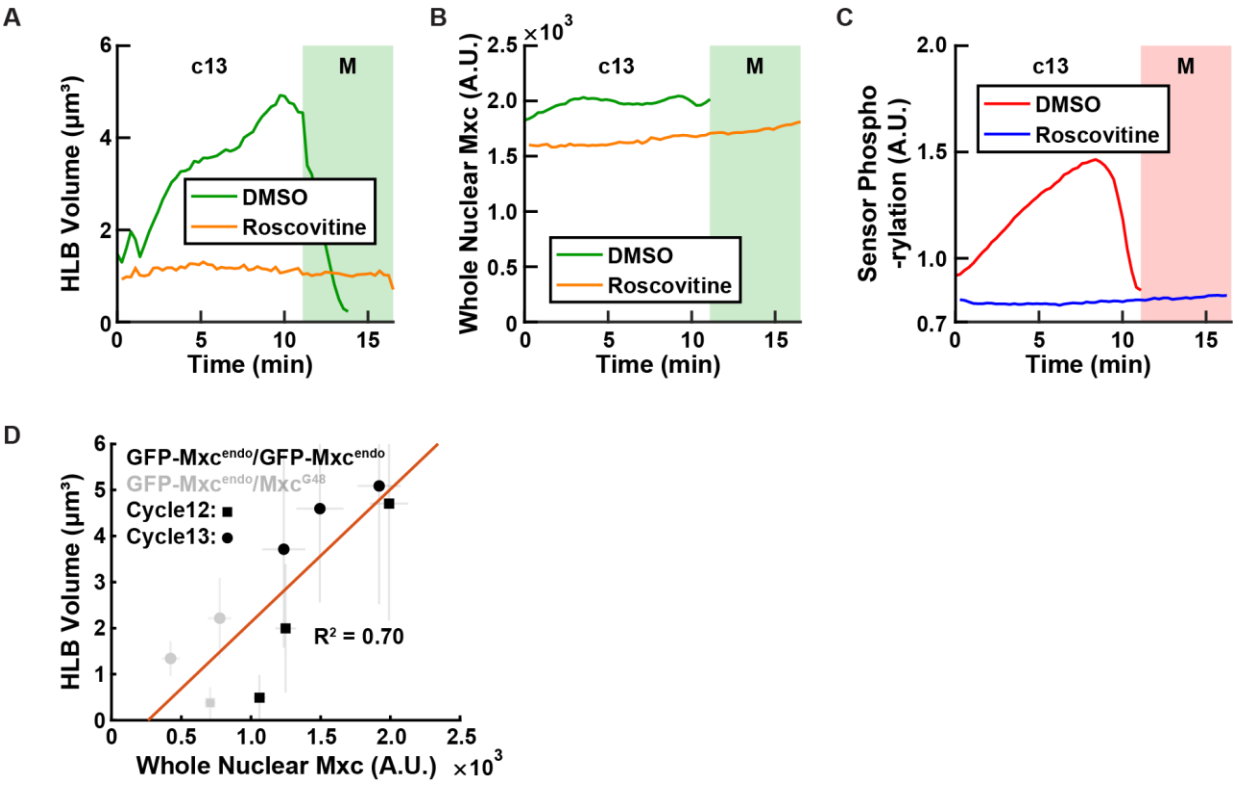

Figure S6. Phase separation of Mxc is dependent on its nuclear concentration, Related to Figure 6

(A) HLB volume during cycle 13 for DMSO control (N=3) and roscovitine injected (N=3) embryos. (B) Nuclear Mxc concentration during cycle 13 for DMSO control (N=3) and roscovitine injected (N=3) embryos. (C) Cdk sensor phosphorylation level during cycle 13 for DMSO control (N=3) and roscovitine injected (N=3) embryos. Notice how roscovitine injected embryos have very low readout from the biosensor (C), are arrested in interphase with a lower concentration of Mxc (B), which is still above threshold so that small HLB persist in the absence of Cdk activity (A). (D) HLB size and nuclear Mxc concentration for endogenously tagged GFP-Mxc lines (black: homozygote, grey: hemizygote). Error bars, standard deviation. A.U., arbitrary units. c, cycle. M, mitosis.

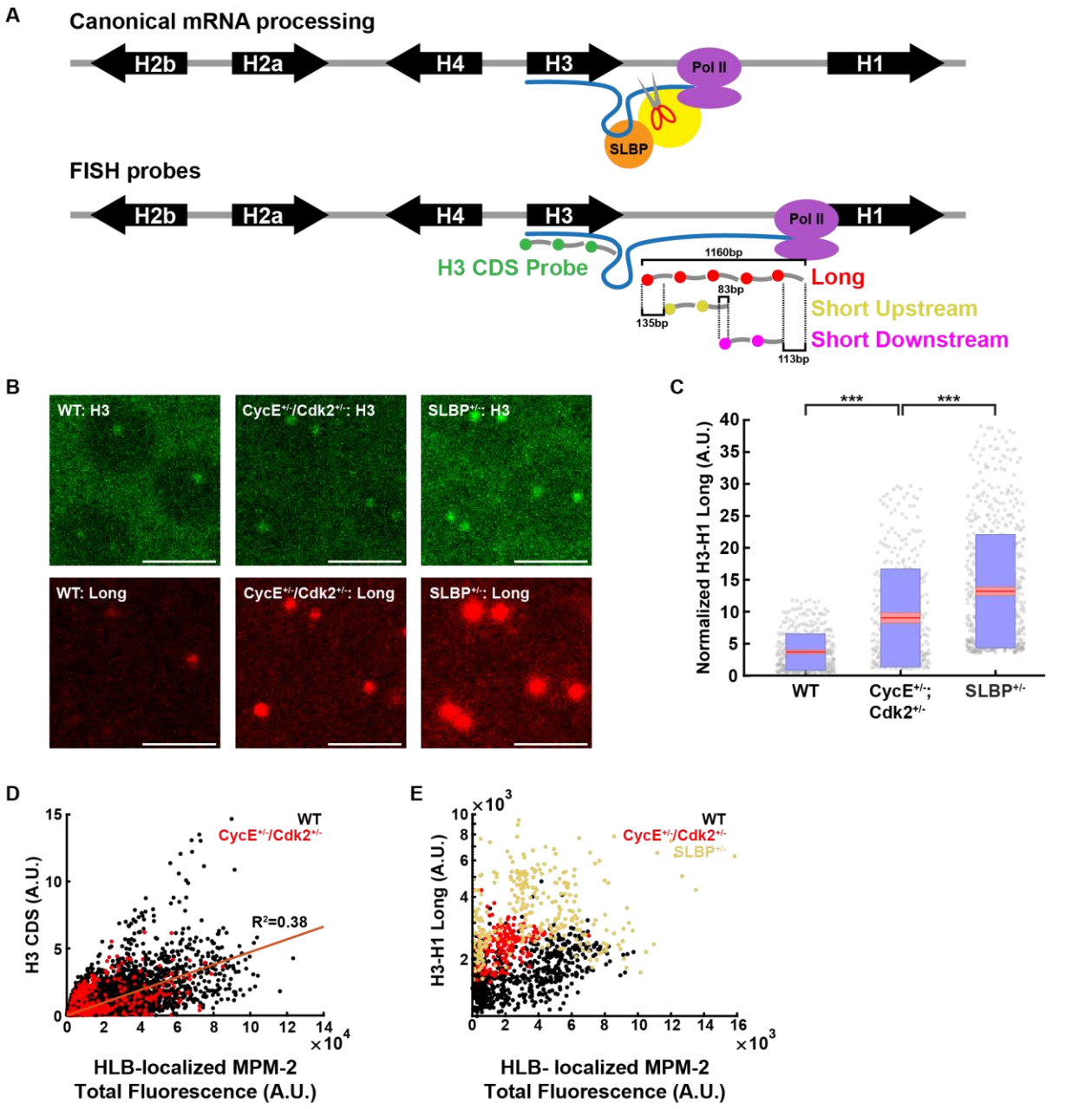

Figure S7. Additional FISH results, Related to Figure 7

(A) Schematic of canonical mRNA processing (top) and the fluorescence in situ hybridization (FISH) probes for histone H3 coding sequence (CDS) and H3-H1 intergenic sequence (bottom). Probes used to detect misprocessing are indicated as 'Long', 'Short Upstream', and 'Short Downstream' probes and target the sequence regions as depicted. The 'Short' probes covered narrower region inside the 'Long' probe target sequence to ensure specificity of the read-through (The 5' end of the 'Short Upstream' probe target sequence was 135 bp downstream of the 'Long' probe target sequence 5' end. The 3' end of the 'Short Downstream' probe target sequence was 113 bp upstream of the 'Long' probe target sequence 3' end.) The 'Short Upstream' and 'Short Downstream' probes had 83 bp overlap. Yellow blob on the top panel is the U7 snRNP bound to the cleavage complex. (B) Representative images of fixed embryos stained with the H3 CDS probe and H3-H1 intergenic 'Long' probes (see Figure 7A), for embryos laid by WT, CycE$^{+/-}$

/Cdk2$^{+/-}$, and SLBP$^{+/-}$ mothers. Scale bars, 5µm. (C) Quantification of normalized misprocessed mRNA levels detected by 'Long' probe for embryos laid by WT, CycE$^{+/-}$/Cdk2$^{+/-}$, and SLBP$^{+/-}$ mothers. Normalization was performed by dividing the H3-H1 Long probe fluorescence by the H3 CDS probe fluorescence. Red, 95% confidence interval for the mean. Blue, 1 standard deviation. Statistical analysis was performed by running a one-way ANOVA followed by a Turkey's Pair test ($p<.10^{-4}$ between all pairs). n=409, 343, and 681 HLBs respectively for WT, CycE$^{+/-}$/Cdk2$^{+/-}$, and SLBP$^{+/-}$. (D) Levels of nascent mRNA measured from the H3 CDS probe and HLB-localized MPM-2 total fluorescence, for embryos laid by WT (black) and CycE$^{+/-}$; Cdk2$^{+/-}$ (red) mothers. Orange line is the best fit line through the origin. (E) Levels of total misprocessed mRNA (detected by the 'Long' probe) level and HLB-localized MPM-2 total fluorescence for WT (black), CycE$^{+/-}$; Cdk2$^{+/-}$ (red) mothers and SLBP$^{+/-}$ (yellow). A.U., arbitrary units.

REAGENT or RESOURCE	SOURCE	IDENTIFIER
Oligonucleotides		
gBlocks Gene Fragments (for Cdk sensor): CATCCAGATTGGGACAATGACCAATGATGTGACTTG GTCCGAGGCCTCCTCGCCAGACGAGCGCACTCTCA CCTTCGCCGAGCGTTGGCAGCTGAGCAGCCCCGAC GGTGTTGACACCGACGATGATCTCCCCAAGTCCCG CGCCTCCAAGCGCACCTGCGGTGTCAACGATGACG AGTCGCCGTCCAAGATCTTCATGGTCGGCGAGTCC CCCCAGGTGTCCTCCCGCCTGCAGAACTTGCGTTT GAACAACTTGATTCCCCGTCAGCTGTTCAAGCCCAC CGACAACCAGGAGACCACTAGTGTGTCCAAGGGCG A	Integrated DNA Technologies, Inc	N/A
Stellaris® FISH probes: H3 CDS probe (reverse compliment): ATGGCTCGTACCAAGCAAACTGCTCGCAAATCGACT GGTGGAAAGGCGCCACGCAAACAACTGGCTACTAA GGCCGCTCGCAAGAGTGCTCCAGCCACCGGAGGT GTGAAGAAGCCCCACCGCTATCGCCCTGGAACCGT GGCCTTGCGTGAAATTCGTCGCTACCAAAAGAGCA CCGAGCTTCTAATCCGCAAGCTGCCTTTCCAGCGTC TGGTGCGTGAAATCGCTCAGGACTTTAAGACGGAC TTGCGATTCCAGAGCTCGGCGGTTATGGCTCTGCA GGAAGCTAGCGAAGCCTACCTGGTTGGTCTCTTCG AAGATACCAACTTGTGTGCCATTCATGCCAAGCGTG TCACCATAATGCCCAAAGACATCCAGTTAGCGCGAC GCATTCGCGGCGAGCGTGCTTAA	Biosearch Technologies, Inc., Petaluma, CA	N/A
Stellaris® FISH probes: H3-H1 intergenic short upstream (reverse compliment): TTGTTCTTTGTGCGAACATCCTTTAAAGCAGTGAAA GTGTCGTGCGGGGCAAGGGACTCTGAACCTTAAAC ATCTAAAAAAAAAAATCTGAATTCTGTGTAAGACAGTT TGAAATTAATGAAATTACATTGATGACGGCAATATTT ATAAAATAACAGAAAATAATAAAATAAAACTAGCTAT TTTATATTTTTTCCATGTGTTAACTGAAGAATGTGTT ATTATTGAAGAGGTCGTACGGGACAATTGACACTGT CCCTTCAAACGTCTGTAAAAAATAAAACCTATGTAAA ATTCAGCACGGAAATTGGCTAATTTTGTTGCGGAAT GTAATATATATTACATAATAAAGGATAATACAAAAAT TGTTTCTTTTTATTTTTTATTTGATTTATTTATTTGACT ACATAGACGGTAATGCATATGTGGCGAGGAAATCG ATTGATTTCAGAACAAATTATTTTAAAATATGCATGA AAACACATTAATAACAAGCAAACA	Biosearch Technologies, Inc., Petaluma, CA	N/A

Stellaris® FISH probes: H3-H1 intergenic short downstream (reverse compliment): TAATGCATATGTGGCGAGGAAATCGATTGATTTCAG AACAAATTATTTTAAAATATGCATGAAAACACATTAA TAACAAGCAAACACATTAATAATTTAAGAAAATATTA TTTATTATATTAATATTATGTTATTTAAGAAAGTATCT GTATTTTTAACGATCGAAAATTATTTCTGAATGCTGC TTTAAAGCAAATTTTTCTGTAGTTCAATGTGAACTTA AATCAAGTAATAAAGTATCTTAATTAATAATAGACGC TTCTTTTAGAAGCCCTTCAAGGGGATGAACGTTTCA ATTTTAATAAACATTACGAATTAGTGAAATATTTGCA ATGATTCTTATTTTATTAGATGTTTTTTTATAAATTGG TCCAGTTAAAAATTTGAATATAAAAATTCAATCAACA TTTGAAAGTCTCAAAACCCATATTACATCCTTTTAAA AATGGAAAGTGACGAAAAAATTATTTAAAAGTGTAG AACTATTAAAACCTTATTTT	Biosearch Technologies, Inc., Petaluma, CA	N/A
Stellaris® FISH probes: H3-H1 intergenic long (reverse compliment): TAAATCATATGTAAAAATACTAATTCTGCCAGAGAAG GAATAAAAATAATCTTATTTTAATTGTAAGCTCGACA TTTATTAAATTAAAGAAGAGGTTAATAAATATAAAATA TATATAAAAATATATATTTTTATTTGTTCTTTGTGCGA ACATCCTTTAAAGCAGTGAAAGTGTCGTGCGGGGA AAGGGACTCTGAACCTTAAACATCTAAAAAAAAAAT CTGAATTCTGTGTAAGACAGTTTGAAATTAATGAAAT TACATTGATGACGGCAATATTTATAAAATAACAGAA AATAATAAAATAAAACTAGCTATTTTATATTTTTTCCA TGTGTTAACTGAAGAAAGTGTTATTATTGAAGAGGT CGTACGGGACAATTGACACTGTCCCTTCAAACGCCT GTAAAAAATAAAACCTATGTAAAATTCAGCACGGAA ATTGGCTAATTTTGTTGCGGAATGTAATATATATTAC ATAATAAAGGATAATACAAAAATTGTTTCTTTTTATTT TTTATTTGATTTATTTATTTGACTACATAGACGGTAAT GCATATGTGGCGAGGAAATCGATTGATTTCAGAAC AAATTATTTTAAAATATGCATGAAAACACATTAATAA CAAGCAAACACATTAATAATTTAAGAAAATATTATTT ATTATATTAATATTATGTTATTTAAGAAAGTATCTGTA TTTTTAACGATCGAAAATTATTTCTGAATGCTGCTTT AAAGCAAATTTTTCTGTAGCTCAATGTGAACTTAAAT CAAGTAATAAAGTATCTTAATTAATAATAGACGCTTC TTTCAGAAGCCTTCTAGGGATGAACGTTTCAATTTTA ATAAACATTACGAATTAGTGAAATATTTGCAATGATT CTTATTTTATTAGATGTTTTTTTATAAATTGGTCCAGT TAAAAATTTGAATATAAAAATTCAATCAACATTTGAAA GTCTCAAAACCCATATTACATCCTTTTAAAAATGGAA AGTGACGAAAAAATTATTTAAAAGTGTAGAACTATTA AAACCTTATTTTTATTAATGATTTAAAATACTAAAAAA TTAAAAAAAGTTTACACTTCAAGCAAACTTCGACATA GTAAATGACTGATGTCAGTAGCATTGTTAAAGTGCT CTCCTCCTCGATTC	Biosearch Technologies, Inc., Petaluma, CA	N/A

Genewiz sfGFP-MXC HDR template: TGCCTGCAGGTCGACTCTAGAGGATCCCCGTAAAA GAATAACATGATCAGTGTTATGTTGGCTGGTGAGCC AACCTTAGCTACTCACATGGATCCTGCTCTACGTAG CGCCGAAGGAAGCGATCCTTGCTCAAGTTGGCGTC ACCGAAGTAGAATTCCATTTGACCGCGAATCGAATT GAACAAATGCCTCTTCCTTTTGCGTCCACCATCCTT TTTATCCGGCGATGCGTCTTCCGGCGCCGGTTCTTT GGAATTTTCCTCAGCTGGTTCAGTGGGTGCGGCTG GATCGGGTTTCTCCGCTGATGTCGCGGGCTCCTGA CCCTCGCCCTTCTCCTTCTCGATACTCTTGGCAGCC ATTGAGTGCCAGTTAACCAGTAATCTAAGTCACTCG AATAAAATATTGCACTTGGTTTTTGCGTTCTGATCTA TTTGGCAACGCCGTCTAGTTATGAATTGCTGGGATG CCAGGTATTTGCAGCATTCCCATATCGATAGTTTAA CGAATATCGGATTCTAAGTACTGTAACGTACACATA AAAACGAATTGAAGCAAGACCATCAAAGCAATAAAA ACTGCTATAATTTGTTTTAAGCGAAAGAGACGTATTT CTTTGCTTTAATTATTACCATTATTTCCCACGCTCCT AATAAGGCTTGGCAGCCAAGCGCAAACAACGGGAC TATATCGATAGTTCGGCGCTGTGGCAACCCTACTGC GTTGTTTTGGCGGGCGGCAAAAAAAACACAGATGC TATGCTAACCTATGTGTGTTGTACAGTGCGCCGCTA GAATCGGCAACAACAAAACGAAAATAGTCGGCGAAT AGGCGAGAAAATGGTTTATTCTCTCTCGAATTAAAG CGCTGATTCAATTCCGACTAACTATTGAGTGATTAAA CCTGCAACAGTCAATAATAAGGCATTACAAGTGCGT TCGATAAACCTAAAGTCTTGCAAGCGAAAAAAAAAA GAAAGGCAAGGCGAAAAGCGAGTGGATGGTGACG CTTAGCTGAGTCGGAAAGTCCAGCCATGGTGTCCA AGGGCGAGGAGCTGTTCACCGGCGTGGTGCCCAT CCTGGTGGAGCTGGATGGCGACGTGAACGGCCAC AAGTTCAGCGTGCGCGGCGAGGGCGAGGGCGACG CCACCAACGGCAAGCTGACCCTGAAGTTCATCTGC ACCACCGGCAAGCTGCCCGTGCCCTGGCCCACCCT GGTGACCACCCTGACCTACGGCGTGCAGTGCTTCA GCCGCTACCCCGATCACATGAAGCAGCACGATTTC TTCAAGAGCGCCATGCCCGAGGGCTACGTGCAGGA GCGCACCATCAGCTTCAAGGATGACGGCACCTACA AGACCCGCGCCGAGGTGAAGTTCGAGGGCGATAC CCTGGTGAACCGCATCGAGCTGAAGGGCATCGATT TCAAGGAGGATGGCAACATCCTGGGCCACAAGCTG GAGTACAACTTCAACAGCCACAACGTGTACATCACC GCCGATAAGCAGAAGAACGGCATCAAGGCCAACTT CAAGATCCGCCACAATGTGGAGGATGGCTCCGTGC AGCTGGCCGATCACTACCAGCAGAACACCCCCATC GGCGACGGCCCAGTGCTGCTGCCCGATAACCACTA CCTGAGCACCCAGAGCGTGCTGTCCAAGGACCCCA ACGAGAAGCGCGATCACATGGTGCTGCTGGAGTTC GTGACCGCCGCCGGCATCACCCTGGGCATGGATGA GCTGTACAAGCACCGGTATACCAGCTTGTACAAAAA GGCGGGAAGCGCAGCGGCCCCATTTACTATGGAGT CGATTGTCCTGCATTCGGACGTTGCTCGCTTGGTCC TGGGTAGGTTTTCCCTGGACGCTTTTCTAGCTCGCA ATATTTATGCTCTTCCATTTTGTAGGCTACCTAGTCA ACCAGAATCTAAAAAGGGCCGCACACACTCTGTGTC	GENEWIZ Global Headquarters & NJ Lab South Plainfield, NJ	N/A

GCACATCGCCTCACCTGCGCCACGAGTTCCTGGCC CTTAAACAGGGCCTGCAGACGCACAACTTCCTTCAC GGGGGTCTGGAGGAGATAATCTGCGAGCATGTCAA GATCACAAGCTTGGGTAAATTAGCACGCTCCTTGCG TTTCTTTTTTTTTGCGGCTGACCGAAAATCTCTCTTT TCAGTGGCCGGTGCCGTGCAGAAGCTGCCGCTGG ATATGCGTATGCAGCTGCAGCAGATGAAGCTGTCC GAACGGGTCAGCGAACTGATAGCCGCCGGCGAGA GGAGTAGCTGTACCAATGAAAGCAGCACCCCAGGC GAGCCCACCATATCACAGTCGCATCGCAAGAGAAG GCGCTTGTAATTATAGATTTTTCCTTGACACAAGCAC ATCGGAATTCTCATTGCTCTCTTACCCCTTTTCCCCA GGCGCACCCATTCTCCCGTGAACAGCATTTCTTCGC CTTCGTTTAGCAAGCGACCGCGTCTGCTGCCGCCA CACTTCTACTGCAGCGTTAACCGCGACAAGGTCAG GCAGAGTTTCCTAGGCAGCCAGGATGACTGCGAGG CGGAACTGGACGAAGAGGATGGCGAGAGCACAAC GGCCACCGAGGACTTGGAGGAGGATGACTTACTTC CGGCGAATGGTCCTGGTCCGCGCAACAATTCCACG CCGCGCCAAGGTCATACCGAGTCCAATCCACTTCT GCTCACGCCGCAAAGCATGCCTGTAAGTCCATAGA CATGCTTAATGCATATCTGCTTAATTAACCAATAGTG CATCTATTATGTATTCTAAACAAAAAACACTCTTTCG ATTTACATTGATTTCAGGAACTGGCCTGCGCGATGG GTACCGAGCTCGAATTCACTGGCCGTC		
Genewiz Guide RNA construct: CTTTTTTGCTCACCTGTGATTGCTCCTACTCAAATAC AAAAACATCAAATTTTCTGTCAATAAAGCATATTTATT TATATTTATTTTACAGGAAAGAATTCCTTTTAAAGTG TATTTTAACCTATAATGAAAAACGATTAAAAAAAATA CATAAAATAATTCGAAAATTTTTGAATAGCCCAGGTT GATAAAAATTCATTTCATACGTTTTATAACTTATGCC CCTAAGTATTTTTTGACCATAGTGTTTCAATTCTACA TTAATTTTACAGAGTAGAATGAAACGCCACCTACTC AGCCAAGAGGCGAAAAGGTTAGCTCGCCAAGCAGA GAGGGCGCCAGTGCTCACTACTTTTTATAATTCTCA ACTTCTTTTTCCAGACTCAGTTCGTATATATAGACCT ATTTTCAATTTAACGTCGGATTGTCCTGCATTCGGA CGGTTTTAGAGCTAGAAATAGCAAGTTAAAATAAGG CTAGTCCGTTATCAACTTGAAAAAGTGGCACCGAGT CGGTGCTTTTTTGCCTACCTGGAGCCTGAGAGTTGT TCAATAAAATAAAAATGTTTCGTTTTTTTGCTTTCGC CAGTATTTATTATTTTT	GENEWIZ Global Headquarters & NJ Lab South Plainfield, NJ	N/A
Primer for mCherry fragment, Forward: CACTAGTGTGTCCAAGGGCGAGGAGC	This paper	N/A
Primer for mCherry fragment, Reverse: GCTGGGGATCCAGATCCACTACTTGTACAGCTCGT CCATGC	This paper	N/A
GFP insertion screening primers to Mxc locus, Forward: AATAGTCGGCGAATAGGCGAGA	This Paper	N/A
GFP insertion screening primers to Mxc locus, Reverse: TATTGCGAGCTAGAAAAGCGTCC	This paper	N/A

Supplementary Table S1. Oligonucleotides used in this study. Related to Key Resources Table.